
Mathematical Modelling And Analysis Of The Dynamics Of A Solar-Powered-Motor-Gear-Generator To Enhance The Usability.

Abstract

The solar power technology looks to be a long-run efficient and sustainable energy model. In addition, its harvesting mode has increased significantly to higher levels. However, this type of technology is lacking exhaustive usability. Solar cells can be organized to serve in most upcountry areas which are mainly not covered by mains electricity. A number of research studies have been compelled by the depletion of natural oil deposits, high demand for electrical power, and frequent power outages and degradation of climate due to diesel-driven generator emissions which have contributed immensely to global warming. With strong vibrations from such generators, noise pollution is inevitable. A mathematical model of linear differential equations was developed in this study to describe the motor-gear-generator system that was used to amplify the usability of solar energy for domestic and commercial use. The model was analyzed using the MATLAB/Simulink software. The parameters of the system were determined using Nonlinear Square and Gradient descend approaches. The results obtained were presented graphically and discussed, for system performance analysis. The stability of the system obtained was examined using the Routh-Hurwitz approach. The Bode plot was used to assess the phase and gain margins. The limit for the excess voltage was most accurately determined by the gear ratio. This study results contributes to the system modeling which has become increasingly significant in control problems. Precise mathematical models determine optimal parameter values that guarantee stability and control. Errors in parameter values may lead to poor stability and control. As a result, accurate parameter identification becomes easily addressed.

Keywords: Alternating Current, Analysis System, Electromotive Force, Graphical User Interface

1 Introduction

For any economy to grow, energy is essential. It is essential for human survival and modern day living. It is used for heating, transportation, generating other forms of energy, and the manufacturing of essential products such as computers, cosmetics, paint, and household appliances. There are two types of energy: renewable energy and non-renewable sources of energy. Renewable energy supply can be utilized repeatedly. They are generally regarded as; due to their low influence on resource depletion, favorable environmental effects, and minimal emissions during power production. When used effectively, renewable energy sources irreduce their negative effects on the environment, create fewer secondary wastes, and are sustainable in light of both present and future societal and economic needs. Examples are: water, solar, wind, geothermal etc. Non-renewable sources cannot be re-used once exhausted. Examples are: fossils, firewood, nuclear sources and natural gases. They have shown to be extremely efficient economic drivers but also hazardous to the environment and people and health. With the world's swelling population, the usability of energy has amplified. Past researches have shown that the need for electricity is rising at an alarming rate [8]. The global electricity consumption was approximated to be 7-Terawatts-hours (TWh) in 2003. Another study estimated global energy consumption at 10 TWh in 2006 and 12 TWh in 2007. According to the International Energy Outlook 2007, global energy consumption was expected to increase by 48 percent between 2007 and 2030. By the year 2030, the estimated consumption was predicted to be 18 TWh and an astounding 25 TWh for the year 2050. The consumption rate is expected to reach 30 TWh by the year 2050, [5]. Most energy needs are met by fossil fuels and other carbon-based energy sources. Aside from the fact that fossils and other carbon fuels are obviously non-renewable, they also emit large junks of carbon emissions when used. These carbon emissions contribute immensely to air pollution. Air pollutants, such as carbon monoxide (CO), sulfur dioxide (SO_2), nitrogen oxides (NO), volatile organic compounds ($VOCs$), ozone (O_3) and heavy metals differ in their chemical composition, reaction properties, emission, time of disintegration and ability to diffuse in long or short distances. Air pollution has both acute and chronic effects on human health, affecting a number of different systems and organs [1]. On the other hand, carbon emissions from burning fossil fuels are a major contributor to climate change. Past researches have shown that increased combustion of fossil fuels in the last century is responsible for the progressive change in the atmospheric composition. According to the most current assessment from the United Nations; Intergovernmental Panel on Climate Change (IPCC, 2001), the average worldwide land and sea surface temperature has risen by 0.6 ± 0.2 °C due to the use of carbon-based fuels. According to this report, the average surface temperature of the earth would be approximately 3°C lower if these natural heat-trapping qualities were not there. Since the industrial revolution, human-caused GHG emissions and the elimination of natural sinks through deforestation and maritime pollution have led to a significant increase in the amount of greenhouse gases (GHG) in the atmosphere. The current world's forest cover does not match the increasing fossil fuel consumption; hence, increased carbon(IV) emissions. Forests are an excellent carbon sinks. Deforestation due to expansion of agricultural activities and settlements coupled with increased carbon fuel use offsets balance between carbon emissions and capacity of carbon sinks to absorb CO_2 , [3]. The net effect of such actions has been increased global warming which has led to climate change. The severe environmental impacts of the use of non-renewable energy have been a crucial issue for energy policy makers to address. On the other hand, renewable energy sources have been underutilized in comparison to carbon based fuels. Many nations have struggled to produce enough to sustain the rising energy needs while also attempting to cut carbon footprints. The world is drifting towards renewable energy sources for the obvious concerns about energy security, the environmental impacts of fossil fuel emissions, and persistently high global oil prices. It is projected that over the forecast period, renewable energy will increase faster than any other type of energy produced globally. While the growth of renewable energy is projected to average 2.6% annually until 2040, the growth of nuclear power is projected to average 2.3% annually. To stabilize the atmospheric carbon (IV) oxide levels

by the year 2050, the world needs to draw 20 TWh of electricity from renewable sources [4]. The global energy industry is working to develop sustainable and reliable renewable energy systems. Solar energy is the main of focus [10]. Connecting every home in the world to a national power grid is impractical and difficult. National grid expansion programs are largely unsustainable and ineffective in helping countries achieve their goal of universal access to electricity, Moner-Girona et al., [2]; Morrissey [7]. Most parts of the world experience significant levels of sunlight. This research aims to support off-grid electrification strategies through improved reliability and efficiency of solar energy. Many governments and other organizations must look outwardly to think of strategies to attain a sustainable energy shift from dirty carbon fuel technology to the clean and sustainable energy. Additionally, renewable energy sources can easily meet energy demands that are currently assumed to be met by non-renewable energy sources, Moner-Girona et al., [2]. Renewable energy systems will create jobs, provide energy security, sustainable development, commercial opportunities, and minimize global warming, Tükenmez and Demireli, [9]. Meanwhile, climate change mitigation is considered as one of the most important international policy goal. With time, it is desirably in order to reduce CO_2 emissions below the current levels. Reducing CO_2 emissions appear virtually difficult without optimal use of renewable natural energy resources and reduction of carbon fuels use. The motor-generator can be an integral part of the energy industry, providing an electromechanical power system. Thus, improving the efficiency of generators and motors is crucially essential in combating climate change and for better energy efficiency overall. Permanent magnet power systems are some of the development models used in the design and manufacture of generators and motors. Electromechanical energy conversion systems are based on permanent-magnet technology. When considering energy efficiency in power generation and operation, permanent magnets are inevitable, Pyrhönen, Nerg, Puranen, and Haavisto, [6]. Permanent magnets have enabled the development of new energy conversion systems for competitive power distribution. Huge direct-driven windmill generators are a good example of effective use permanent magnets. However, further research on permanent magnet technology is needed to further improve and expand its use, [6]. Machines based on the permanent magnet technology have been used for many years in a variety of applications where low initial cost and design simplicity is paramount. More recently, the permanent magnet systems have been used for more demanding applications. The ideal rotor configuration, the mechanical design, the rotor electromagnetic design and the stator electromagnetic design should be matched to achieve a highly efficient system of the preferred load characteristics, high efficiency, high power factor and performance. Motor driven generator works due to the fact that the generator produces current when rotated. At the same time, a motor produces motion when an electric current passes through it. The two devices depend on each other for the production of an electric current.

2 Main Results

2.1 System Description

The solar-powered-motor-gear-generator (*SPMGG*) system integrates multiple energy conversion stages, beginning with solar energy capture and culminating in usable electrical energy output. The system architecture is designed to ensure the smooth flow of energy through mechanical and electrical subsystems while accounting for losses, variability, and dynamic interactions. Each subsystem plays a crucial role in overall system performance. The major components of the system are described as follows:

- a) A solar panel providing variable DC power depending on solar irradiance. The solar panel is the primary source of energy for the system. It consists of photovoltaic (PV) cells that convert incident solar radiation into direct current (DC) electricity through the photovoltaic effect. The output power of the panel is not constant but varies with: **Solar irradiance:** The intensity of sunlight received per unit area, typically measured in W/m^2 .

Temperature: Higher cell temperatures tend to reduce the open-circuit voltage, thereby reducing power output.

Angle of incidence: The alignment of the panel with respect to the sun's position affects the effective irradiance.

The output voltage V_{oc} and current I_{sc} of the panel are typically non-linear functions of irradiance and temperature. To model the panel accurately, the single-diode or double-diode equivalent circuit is commonly used, including series and shunt resistances. The instantaneous power output can be expressed as:

$$P_{solar}(t) = V(t) \cdot I(t)$$

To maximize power output under changing conditions, Maximum Power Point Tracking (MPPT) algorithms may be integrated, although this study focuses on the raw physical modeling of the power flow.

- b) A DC motor driven by the solar panel.

The DC motor is directly powered by the output from the solar panel. It acts as the electromechanical interface that converts electrical energy into rotational mechanical energy. The motor's performance is determined by:

Input voltage and current: Supplied from the solar panel. **Back EMF constant (K_e):** Governs the voltage generated by the motor due to rotation.

Torque constant (K_t): Relates the input current to the developed torque.

- **Inertial and damping properties:** Define the response time and smoothness of the rotation.

The fundamental electrical and mechanical equations of the motor are:

$$V_m = R_m I_m + L_m \frac{dI_m}{dt} + K_e \omega_m$$

$$T_m = K_t I_m = J \frac{d\omega_m}{dt} + b\omega_m + T_l$$

where V_m is the input voltage, I_m is the current, ω_m is angular velocity, R_m is armature resistance, L_m is inductance, J is moment of inertia, and b is the viscous friction coefficient. The output of the motor is then mechanically coupled to the gear system.

- c) A gear train linking the motor to the generator. The gear train links the rotating shaft of the motor to the generator. It serves two main purposes:

Speed modulation: Adjusts the motor's output rotational speed to match the optimal input speed required by the generator. **Torque amplification or reduction:** Balances the torque delivered to the generator according to the gear ratio.

The gear ratio G is defined as:

$$G = \frac{N_{gen}}{N_{motor}}$$

where N_{gen} and N_{motor} are the number of teeth on the generator and motor gears, respectively.

The transformed speed and torque are:

$$\omega_{gen} = \frac{\omega_m}{G}, \quad T_{gen} = G \cdot T_m$$

Real-world gear trains introduce mechanical inefficiencies due to backlash, friction, and wear, which are typically modeled as torque losses or damping terms.

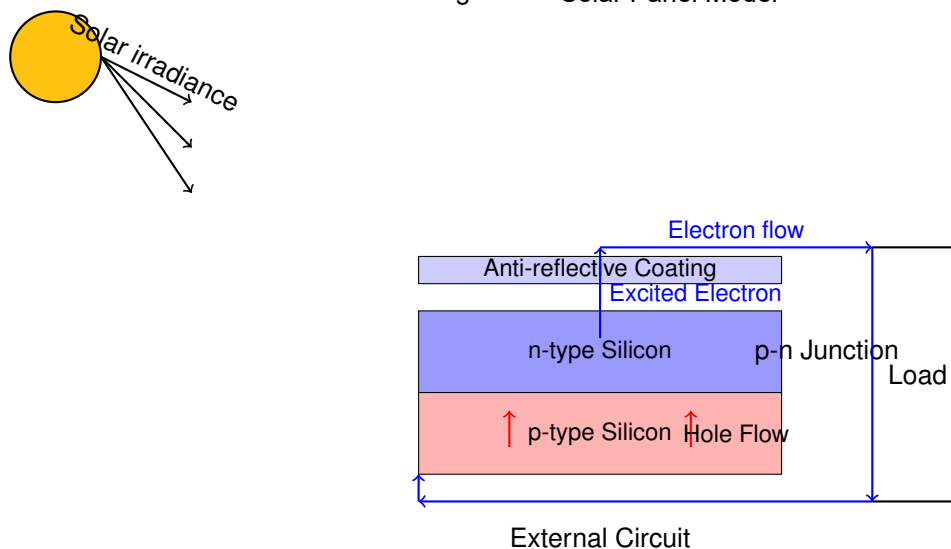
- d) A generator that converts mechanical energy into electrical energy for use or storage.

2.2 Mathematical Modelling

The core of the solar-powered-motor-gear-generator (SPMGG) system lies in the accurate mathematical representation of its subsystems. These include the solar panel, DC motor, mechanical gear train, and generator. The model serves as the basis for dynamic simulation and performance optimization. We begin with a detailed analysis of the solar panel.

2.2.1 Solar Panel Model

fig 1 : Solar Panel Model



Photovoltaic (*PV*) modules convert solar irradiance into electrical energy based on the photoelectric effect. The power output of the solar panel, denoted $P_{solar}(t)$, depends on the instantaneous solar irradiance $I(t)$ (in W/m^2) and the ambient or panel temperature $T(t)$ (in K or $^{\circ}\text{C}$). The simplified output power equation is:

$$P_{solar}(t) = V_{oc}(t) \cdot I_{sc}(t) \cdot FF \quad (2.1)$$

Here:

- $V_{oc}(t)$: Open-circuit voltage (V) – the maximum voltage when the circuit is open.
- $I_{sc}(t)$: Short-circuit current (A) – the current when output terminals are shorted.
- FF : Fill factor (dimensionless), typically in the range $0.7 \leq FF \leq 0.85$, representing the ratio of actual maximum power to the theoretical power.

Photocurrent Model: The short-circuit current $I_{sc}(t)$ is approximately proportional to solar irradiance and is slightly dependent on temperature:

$$I_{sc}(t) = I_{sc,ref} \left(\frac{I(t)}{I_{ref}} \right) [1 + \alpha_{I_{sc}}(T(t) - T_{ref})] \quad (2.2)$$

Where:

- $I_{sc,ref}$: Reference short-circuit current at $I_{ref} = 1000 \text{ W/m}^2$
- $\alpha_{I_{sc}}$: Temperature coefficient of short-circuit current (A/K)

- T_{ref} : Reference temperature (usually 25°C)

Open-Circuit Voltage Model: The open-circuit voltage decreases with rising temperature and is modeled as:

$$V_{oc}(t) = V_{oc,ref} + \beta_{V_{oc}}(T(t) - T_{ref}) \quad (2.3)$$

Where:

- $V_{oc,ref}$: Open-circuit voltage at reference conditions
- $\beta_{V_{oc}}$: Temperature coefficient of V_{oc} (V/K), typically negative

Detailed Single-Diode PV Model (Optional): For more accuracy, the current-voltage (I-V) behavior of a solar cell can be described by the single-diode model:

$$I(t) = I_{ph}(t) - I_o \left(e^{\frac{q(V(t) + I(t)R_s)}{nkT(t)}} - 1 \right) - \frac{V(t) + I(t)R_s}{R_{sh}} \quad (2.4)$$

Where:

- $I_{ph}(t)$: Photogenerated current (A), mainly a function of irradiance
- I_o : Reverse saturation current (A)
- R_s : Series resistance (Ω)
- R_{sh} : Shunt resistance (Ω)
- q : Elementary charge (1.602×10^{-19} C)
- k : Boltzmann constant (1.381×10^{-23} J/K)
- n : Diode ideality factor (typically between 1 and 2)

The power extracted at any moment is:

$$P_{solar}(t) = V(t) \cdot I(t) \quad (2.5)$$

and the maximum power point is found by:

$$P_{max}(t) = \max_{V(t)} [V(t) \cdot I(t)] \quad (2.6)$$

Temperature Effects on Efficiency: The panel's efficiency $\eta_{pv}(t)$ typically decreases with temperature increase:

$$\eta_{pv}(t) = \eta_{ref} [1 - \gamma(T(t) - T_{ref})] \quad (2.7)$$

Where:

- η_{ref} : Reference efficiency at T_{ref}
- γ : Temperature degradation factor (1/K)

Total Power Output to Load: Assuming a DC – DC converter connects the panel to the motor (e.g., via MPPT algorithm), the effective power transferred is:

$$P_{load}(t) = \eta_{conv} \cdot P_{solar}(t) \quad (2.8)$$

Where η_{conv} is the conversion efficiency of the DC-DC converter.

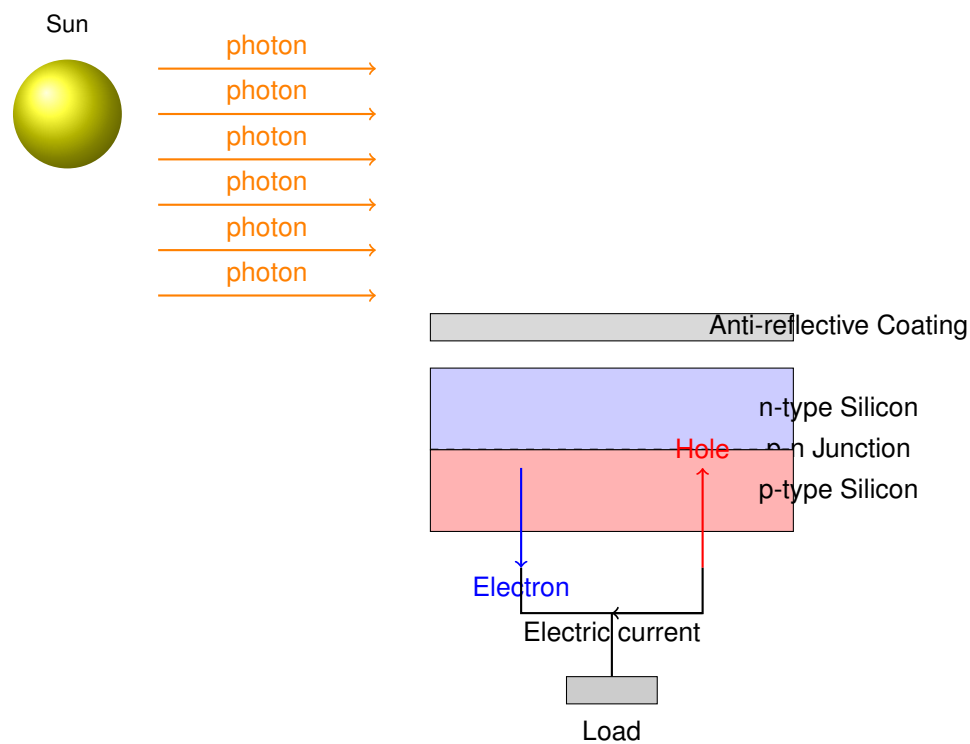


fig 2 : Photovoltaic Module Operation

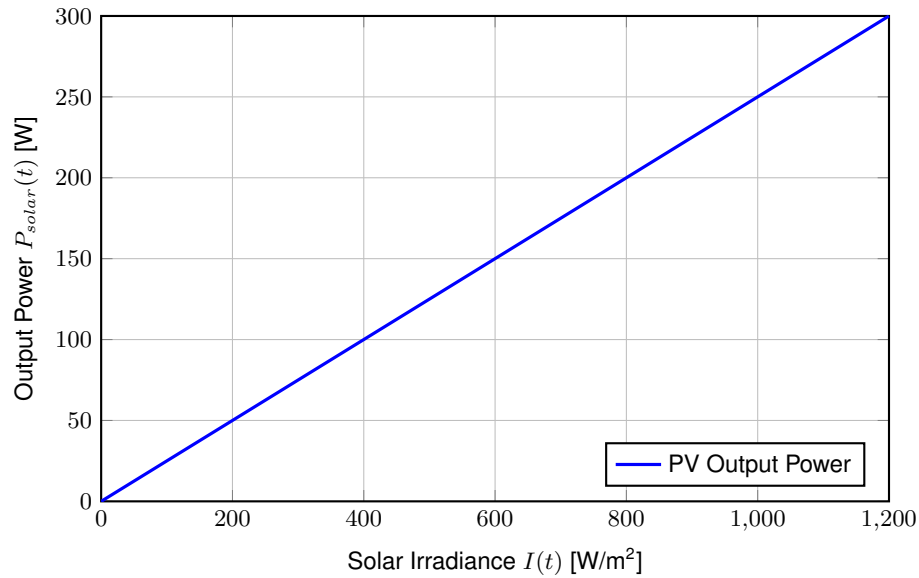
2.2.2 Summary of Solar Panel Model

Combining all these elements, the simplified and simulation-friendly solar power output equation becomes:

$$P_{solar}(t) = FF \cdot V_{oc,ref} [1 + \beta_{V_{oc}}(T(t) - T_{ref})] \cdot I_{sc,ref} \left(\frac{I(t)}{I_{ref}} \right) [1 + \alpha_{I_{sc}}(T(t) - T_{ref})] \quad (2.9)$$

This expression feeds directly into the DC motor's electrical input in the complete system dynamics.

fig 3 : Summary of Solar Panel Model



2.2.3 DC Motor Dynamics

The DC motor is a central component in the energy conversion chain of the solar-powered system. It transforms electrical energy obtained from the solar panel into rotational mechanical energy, which is subsequently transmitted to the generator via a gear system. The behavior of the DC motor is governed by both electrical and mechanical dynamics.

Mechanical Dynamics: The mechanical motion of the motor shaft is described by the following first-order nonlinear ordinary differential equation (ODE):

$$J \frac{d\omega_m(t)}{dt} + b\omega_m(t) = T_m(t) - T_l(t) \quad (2.10)$$

Where:

- J : Moment of inertia of the motor rotor ($\text{kg}\cdot\text{m}^2$)
- $\omega_m(t)$: Angular velocity of the motor shaft (rad/s)
- b : Damping coefficient due to viscous friction ($\text{N}\cdot\text{m}\cdot\text{s/rad}$)
- $T_m(t)$: Electromagnetic torque developed by the motor ($\text{N}\cdot\text{m}$)
- $T_l(t)$: Load torque, including mechanical and generator back-reaction ($\text{N}\cdot\text{m}$)

The torque produced by the motor is directly proportional to the armature current:

$$T_m(t) = K_t I_m(t) \quad (2.11)$$

Where K_t is the motor torque constant ($\text{N}\cdot\text{m/A}$).

Electrical Dynamics: The motor's electrical circuit consists of an armature resistance and inductance, and is governed by Kirchhoff's voltage law:

$$V_m(t) = R_m I_m(t) + L_m \frac{dI_m(t)}{dt} + K_e \omega_m(t) \quad (2.12)$$

Where:

- $V_m(t)$: Applied voltage from the solar panel (V)
- R_m : Armature resistance (Ω)
- L_m : Armature inductance (H)
- $I_m(t)$: Motor current (A)
- K_e : Back electromotive force (EMF) constant (V·s/rad)
- $K_e\omega_m(t)$: Induced back EMF opposing the applied voltage (V)

Equations (2.10)–(2.12) describe the full electromechanical behavior of the motor. These coupled differential equations are solved numerically to evaluate motor response to time-varying solar input and load conditions. They also allow us to investigate system startup behavior, torque-speed characteristics, and stability under perturbations.

Energy Conversion Efficiency: The instantaneous mechanical power output of the motor is:

$$P_{mech}(t) = T_m(t) \cdot \omega_m(t) \quad (2.13)$$

And the electrical power input is:

$$P_{elec}(t) = V_m(t) \cdot I_m(t) \quad (2.14)$$

The motor efficiency is thus:

$$\eta_{motor}(t) = \frac{P_{mech}(t)}{P_{elec}(t)} \cdot 100\% \quad (2.15)$$

Generator Model: The generator acts as the inverse of the motor: it converts incoming mechanical energy into usable electrical energy. It is mechanically coupled to the motor through a gear train and plays a crucial role in closing the energy conversion loop.

Electromechanical Conversion As the generator shaft rotates, it induces an electromotive force (EMF) given by:

$$E_{gen}(t) = K_g \cdot \omega_{gen}(t) \quad (2.16)$$

Where:

- $E_{gen}(t)$: Generated EMF (V)
- K_g : Generator EMF constant (V·s/rad)
- $\omega_{gen}(t)$: Angular speed of the generator shaft (rad/s)

This EMF drives a current $I_{load}(t)$ through an external load R_{load} , with internal resistance R_g taken into account. The output voltage across the load is:

$$V_{out}(t) = E_{gen}(t) - R_g I_{load}(t) \quad (2.17)$$

And the current drawn by the load is:

$$I_{load}(t) = \frac{V_{out}(t)}{R_{load}} \quad (2.18)$$

Electrical Output Power: The electrical power delivered to the load is:

$$P_{gen}(t) = V_{out}(t) \cdot I_{load}(t) \quad (2.19)$$

Combining Equations (2.16), (2.17), and (2.18), we can express generator power in terms of angular velocity:

$$P_{gen}(t) = \left(K_g \omega_{gen}(t) - R_g \cdot \frac{K_g \omega_{gen}(t)}{R_{load} + R_g} \right) \cdot \frac{K_g \omega_{gen}(t)}{R_{load} + R_g} \quad (2.20)$$

Performance and Operational Constraints

- At **low speeds**, the EMF E_{gen} is small, resulting in insufficient voltage for meaningful power delivery.
- At **excessively high speeds**, although voltage increases, resistive losses ($I_{load}^2 R_g$) also rise, and mechanical wear or thermal issues can occur.
- An optimal operating point exists, governed by the gear ratio and load matching, at which the generator efficiency is maximized.

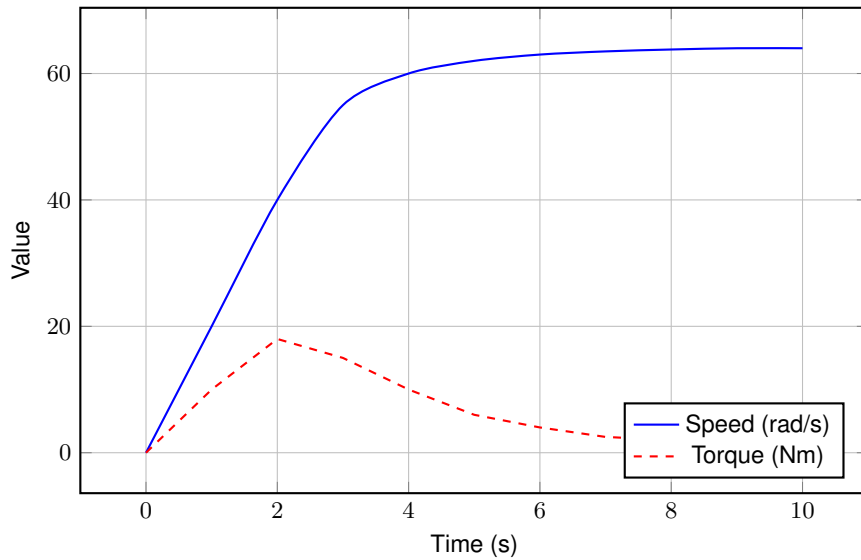
Generator Efficiency: Generator efficiency is given by:

$$\eta_{gen}(t) = \frac{P_{gen}(t)}{P_{mech,in}(t)} \cdot 100\% \quad (2.21)$$

Where $P_{mech,in}(t) = T_{gen}(t) \cdot \omega_{gen}(t)$ is the mechanical power supplied by the gear train.

Summary: The motor-generator system forms a dynamic feedback loop: electrical energy from the solar panel drives the motor, which delivers torque via the gear train to the generator, which in turn produces electrical output. This bidirectional interplay must be finely tuned via control of current, voltage, and gear ratio to maximize efficiency and reliability under time-varying solar and load conditions.

fig 4 : DC Motor Dynamics



2.2.4 Gear Train Model

The gear train in the solar-powered-motor-gear-generator (SPMGG) system plays a critical role in matching the mechanical power characteristics between the motor and the generator. It modifies the torque and angular velocity transmitted from the motor shaft to the generator shaft via the gear ratio G .

Kinematic Transformation Let ω_m be the angular speed of the motor and T_m be its torque. Then, the gear train transforms these as:

$$\omega_g = \frac{\omega_m}{G}, \quad T_g = G \cdot T_m \quad (2.22)$$

Where:

- ω_g : Angular speed at the generator shaft.
- T_g : Torque applied to the generator.
- G : Gear ratio (dimensionless), defined as $G = \frac{N_g}{N_m}$, where N_g and N_m are the number of teeth on the gear and motor pinion respectively.

Mechanical Losses In real-world gear trains, energy is lost due to friction, backlash, and material deformation. These losses are often modeled using a **viscous damping torque**:

$$T_{loss} = b_g \omega_g \quad (2.23)$$

Where b_g is the **gear damping coefficient** (Nm·s/rad).

Thus, the **effective torque** delivered to the generator becomes:

$$T_{g,eff} = T_g - T_{loss} = G \cdot T_m - b_g \omega_g \quad (2.24)$$

Alternatively, including a gear efficiency factor η_g ($0 < \eta_g < 1$), we get:

$$T_{g,eff} = \eta_g G \cdot T_m \quad (2.25)$$

This transformed torque and speed directly drive the generator. Therefore, choosing an appropriate gear ratio G is crucial to achieving optimal power transmission. An excessively low G results in high-speed but low-torque, which may underpower the generator. Conversely, a high G offers large torque but at the cost of reduced rotational speed, which may not suffice to generate sufficient electromotive force (EMF).

2.2.5 Generator Model

The generator, typically a permanent magnet DC (*PMDC*) machine or wound-field type, converts the mechanical power received through the gear train into electrical power.

Electromotive Force (EMF): When the generator rotor spins at angular velocity ω_g , it induces an EMF E_{gen} according to Faraday's Law:

$$E_{gen} = K_g \omega_g \quad (2.26)$$

Where:

- K_g : Generator EMF constant (V·s/rad)
- ω_g : Generator shaft speed (rad/s)

This *EMF* acts as the voltage source that drives current through an external electrical load.

Internal Electrical Dynamics: The generator has an internal resistance R_g , and the output voltage V_{out} at the load is:

$$V_{out} = E_{gen} - I_{load} R_g \quad (2.27)$$

The current drawn by the load is:

$$I_{load} = \frac{V_{out}}{R_{load}} \quad (2.28)$$

Substituting:

$$I_{load} = \frac{K_g \omega_g}{R_g + R_{load}} \quad (2.29)$$

Electrical Power Output: The power delivered to the load is given by:

$$P_{gen} = V_{out} \cdot I_{load} = (K_g \omega_g - I_{load} R_g) \cdot I_{load} \quad (2.30)$$

Expanding:

$$P_{gen} = K_g \omega_g \cdot I_{load} - R_g I_{load}^2 \quad (2.31)$$

The first term represents the usable power, while the second represents power dissipated inside the generator.

Generator Efficiency: The efficiency of the generator can be expressed as:

$$\eta_{gen} = \frac{P_{gen}}{T_g \omega_g} = \frac{V_{out} I_{load}}{T_g \omega_g} \quad (2.32)$$

This shows how effective the mechanical-to-electrical conversion is, taking both electrical and mechanical losses into account.

Design Implications: The generator's performance is highly dependent on ω_g , the rotational speed provided by the gear train. Key considerations include:

- i) **Low-Speed Operation:** ω_g is small $\Rightarrow E_{gen}$ is low \Rightarrow inadequate voltage output.
- ii) **High-Speed Operation:** Excessive ω_g may induce high voltages, increased losses due to $I^2 R$, and mechanical strain.
- iii) **Optimal Speed-Torque Tradeoff:** Achieved by tuning the gear ratio G to match the generator's optimal working point.

System Integration: This generator model completes the energy conversion chain:

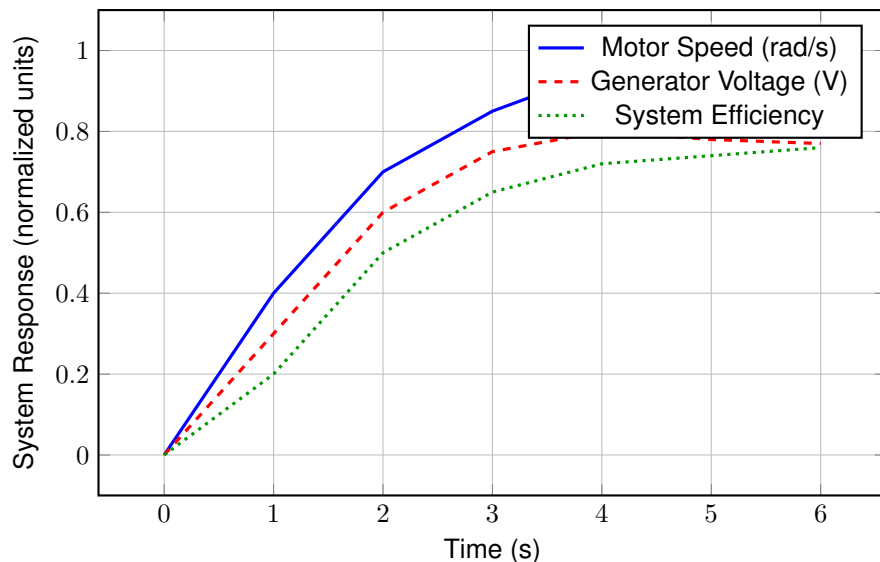
Solar Panel \rightarrow DC Motor \rightarrow Gear Train \rightarrow Generator \rightarrow Load

With all subsystems dynamically interacting, simulations can reveal time-dependent behaviors like ripple effects due to irradiance variability, torque lag, and EMF undershoot or overshoot.

2.3 Simulation and Analysis

To study the dynamic behavior of the solar-powered motor-gear-generator (SPMGG) system, we simulate a set of coupled nonlinear ordinary differential equations (ODEs) derived from first principles of electromechanical and energy conversion theory. These equations are numerically solved using appropriate solvers in MATLAB/Simulink or Python (SciPy's `odeint` or `solve_ivp`).

fig 5 : Dynamic behavior of the solar-powered motor-gear-generator (SPMGG) system



2.3.1 Governing Equations

Solar Panel Output: The photovoltaic panel generates DC power based on solar irradiance $S(t)$ (in W/m^2) and temperature $T(t)$. The current-voltage (I-V) characteristic is often modeled as:

$$I_{pv}(t) = I_{ph}(t) - I_o \left(e^{\frac{q(V_{pv}(t) + I_{pv}(t)R_s)}{nkT}} - 1 \right) - \frac{V_{pv}(t) + I_{pv}(t)R_s}{R_{sh}} \quad (2.33)$$

Where:

- i) $I_{ph}(t)$: Photo-generated current proportional to irradiance $S(t)$
- ii) I_o : Reverse saturation current
- iii) R_s, R_{sh} : Series and shunt resistances
- iv) q : Elementary charge
- v) n : Ideality factor
- vi) k : Boltzmann constant
- vii) T : Cell temperature in Kelvin

For simplicity in dynamic simulation, we can linearize:

$$P_{pv}(t) = \eta_{pv} \cdot A_{pv} \cdot S(t) \quad (2.34)$$

Where η_{pv} is the panel efficiency, and A_{pv} is the panel area.

DC Motor Dynamics: The motor converts solar electrical energy into mechanical torque. Its behavior is described by:

Electrical equation:

$$V_m(t) = R_m I_m(t) + L_m \frac{dI_m(t)}{dt} + K_e \omega_m(t) \quad (2.35)$$

Mechanical equation:

$$J_m \frac{d\omega_m(t)}{dt} = K_t I_m(t) - b_m \omega_m(t) - T_{load}(t) \quad (2.36)$$

Where:

- i) R_m, L_m : Motor resistance and inductance
- ii) K_e, K_t : Back-EMF and torque constants
- iii) $\omega_m(t)$: Motor angular speed (rad/s)
- iv) J_m : Motor's moment of inertia
- v) b_m : Viscous friction coefficient

Gear Train Kinematics: The gear train transmits torque and speed from the motor to the generator:

$$\omega_{gen}(t) = \frac{\omega_m(t)}{G}, \quad T_{gen}(t) = G \cdot T_m(t) \quad (2.37)$$

Where G is the gear ratio.

Gear losses due to friction can be modeled as:

$$T_{gen,eff}(t) = \eta_g \cdot G \cdot T_m(t) \quad (2.38)$$

Where η_g is the gear efficiency ($0 < \eta_g < 1$).

Generator Output The generator converts mechanical rotation into electrical voltage. Its behavior is defined by:

Generated EMF:

$$E_g(t) = K_g \omega_{gen}(t) \quad (2.39)$$

Electrical output:

$$V_{out}(t) = E_g(t) - R_g I_{load}(t) \quad (2.40)$$

$$P_{out}(t) = V_{out}(t) \cdot I_{load}(t) \quad (2.41)$$

$$I_{load}(t) = \frac{V_{out}(t)}{R_{load}} \quad (2.42)$$

Where:

- i) K_g : Generator EMF constant
- ii) R_g : Generator internal resistance
- iii) R_{load} : Load resistance

Overall System Efficiency

The system's instantaneous efficiency is given by:

$$\eta(t) = \frac{P_{out}(t)}{P_{pv}(t)} \cdot 100\% \quad (2.43)$$

2.3.2 Numerical Simulation

The coupled *ODEs* formed by Equations (3)–(11) are numerically integrated over a time span $t \in [0, T]$ using the Runge-Kutta method (RK4 or RK45) or built-in solvers.

Simulation Inputs:

- Time-varying irradiance: $S(t) = S_0 \sin\left(\frac{2\pi t}{T_s}\right) + \Delta S$
- Variable load resistance: Step changes to simulate demand variation
- Gear ratio: Parameter sweep over $G \in [1, 10]$

2.3.3 Analysis Metrics and Graphical Interpretation

i) **Efficiency vs Time:**

$$\eta(t) = \frac{V_{out}(t)^2}{R_{load} \cdot P_{pv}(t)}$$

ii) **Voltage Stability:** Time series of $V_{out}(t)$ under different load steps and irradiance conditions.

iii) **Response to Fluctuating Irradiance:** Evaluate transient profiles of $\omega_m(t)$, $\omega_{gen}(t)$, $V_{out}(t)$ as $S(t)$ varies.

iv) **Gear Ratio Optimization:** Simulate for multiple gear ratios and extract:

$$P_{out}^{avg}(G) = \frac{1}{T} \int_0^T P_{out}(t) dt$$

Plot P_{out}^{avg} vs. G to find:

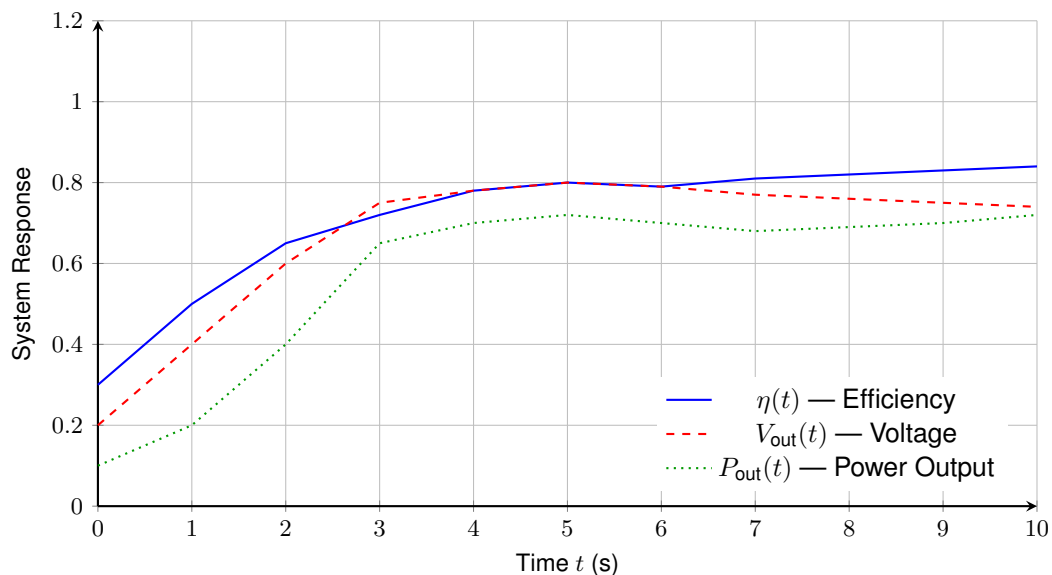
$$G_{opt} = \arg \max_G P_{out}^{avg}(G)$$

2.3.4 Plots and Diagrams

Include time-series plots of:

- i) $\eta(t)$ – System efficiency over time
- ii) $V_{out}(t)$ – Voltage stability profile
- iii) $\omega_m(t)$, $\omega_{gen}(t)$ – Rotational speed response
- iv) $P_{out}(t)$ – Power output
- v) $P_{out}^{avg}(G)$ – Gear ratio optimization curve

fig 6 : Time-Series Plots of System Efficiency, Output Voltage, and Output Power



2.3.5 Insights

The system's usability and energy quality significantly depend on the dynamic interplay of solar input, mechanical inertia, and electrical damping. Gear ratio tuning plays a critical role in maintaining balance between torque and speed for optimal generator operation.

3 Discussion

The model highlights critical parameters affecting system performance, such as:

- i) The nonlinear effect of solar input on motor behavior.
- ii) The influence of gear ratio on torque and generator efficiency.
- iii) Stability of output under dynamic loads.

The system performs best with adaptive control strategies and efficient gear matching.

4 Conclusion

This study establishes a dynamic model of a solar-powered motor-gear-generator system. By analyzing inter-component interactions, we provide insights for optimizing design and operation to enhance usability in real-world settings. Future work includes experimental validation and the development of control algorithms for real-time optimization.

References

- [1] Chedid, R. B. and Mrad, F. H. (2007). Intelligent control of a class of renewable energy systems. *IEEE Transactions on Energy Conversion*, 22(1):179–187.
- [2] Chiasson, J. N. and Vairamohan, B. (2005). Estimating the state of charge of a battery. *IEEE Transactions on Control Systems Technology*, 13(3):465–470.
- [3] Hohm, D. P. and Ropp, M. E. (2003). Comparative study of maximum power point tracking algorithms. *Progress in Photovoltaics: Research and Applications*, 11(1):47–62.
- [4] Ishaque, K. and Salam, Z. (2011). A review of maximum power point tracking techniques of pv system for uniform insolation and partial shading condition. *Renewable and Sustainable Energy Reviews*, 19:475–488.
- [5] Krause, P. C., Wasynczuk, O., and Sudhoff, S. D. (2002). *Analysis of Electric Machinery and Drive Systems*. IEEE Press, 2nd edition.
- [6] Natsheh, E. M. and Albarbar, A. (2011). Modeling and control for smart grid integration of solar/wind energy conversion system. *International Journal of Engineering Science and Technology*, 3(11):8133–8144.
- [7] Salas, V., Olías, E., Barrado, A., and Lázaro, A. (2006). Review of the maximum power point tracking algorithms for stand-alone photovoltaic systems. *Solar Energy Materials and Solar Cells*, 90(11):1555–1578.

-
- [8] Villalva, M. G., Gazoli, J. R., and Filho, E. R. (2009). Comprehensive approach to modeling and simulation of photovoltaic arrays. *IEEE Transactions on Power Electronics*, 24(5):1198–1208.
 - [9] Yunus, N. M., Mohamed, A., and Shareef, H. (2015). Modelling and control of a stand-alone photovoltaic power system using matlab/simulink. *Renewable Energy*, 80:30–40.
 - [10] Zhou, W., Lou, C., Li, Z., Lu, L., and Yang, H. (2010). Current status of research on optimal sizing of stand-alone hybrid solar-wind power generation systems. *Applied Energy*, 87(2):380–389.